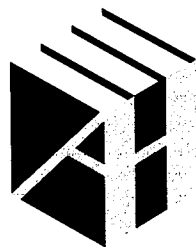


Advances in FDTD Computational Electrodynamics

Photonics and Nanotechnology

Allen Taflove
Editor

Ardavan Oskooi and Steven G. Johnson
Coeditors



**ARTECH
HOUSE**

BOSTON | LONDON
artechhouse.com

Contents

Preface

xv

1 Parallel-Processing Three-Dimensional Staggered-Grid Local-Fourier-Basis PSTD Technique

Ming Ding and Kun Chen

1

1.1	Introduction	1
1.2	Motivation	1
1.3	Local Fourier Basis and Overlapping Domain Decomposition	3
1.4	Key Features of the SL-PSTD Technique	4
1.4.1	FFT on a Local Fourier Basis	4
1.4.2	Absence of the Gibbs Phenomenon Artifact	7
1.5	Time-Stepping Relations for Dielectric Systems	7
1.6	Elimination of Numerical Phase Velocity Error for a Monochromatic Excitation	9
1.7	Time-Stepping Relations within the Perfectly Matched Layer Absorbing Outer Boundary	10
1.8	Reduction of the Numerical Error in the Near-Field to Far-Field Transformation	13
1.9	Implementation on a Distributed-Memory Supercomputing Cluster	14
1.10	Validation of the SL-PSTD Technique	16
1.10.1	Far-Field Scattering by a Plane-Wave-Illuminated Dielectric Sphere	16
1.10.2	Far-Field Radiation from an Electric Dipole Embedded within a Double-Layered Concentric Dielectric Sphere	18
1.11	Summary	19
	References	20

2 Unconditionally Stable Laguerre Polynomial-Based FDTD Method

Bin Chen, Yantao Duan, and Hailin Chen

21

2.1	Introduction	21
2.2	Formulation of the Conventional 3-D Laguerre-Based FDTD Method	22
2.3	Formulation of an Efficient 3-D Laguerre-Based FDTD Method	26
2.4	PML Absorbing Boundary Condition	30
2.5	Numerical Results	33
2.5.1	Parallel-Plate Capacitor: Uniform 3-D Grid	33
2.5.2	Shielded Microstrip Line: Graded Grid in One Direction	35
2.5.3	PML Absorbing Boundary Condition Performance	37
2.6	Summary and Conclusions	38
	References	39

3 Exact Total-Field/Scattered-Field Plane-Wave Source Condition

Tengmeng Tan and Mike Potter

41

3.1	Introduction	41
3.2	Development of the Exact TF/SF Formulation for FDTD	43
3.3	Basic TF/SF Formulation	43
3.4	Electric and Magnetic Current Sources at the TF/SF Interface	44
3.5	Incident Plane-Wave Fields in a Homogeneous Background Medium	45
3.6	FDTD Realization of the Basic TF/SF Formulation	46

3.7	On Constructing an Exact FDTD TF/SF Plane-Wave Source	48
3.8	FDTD Discrete Plane-Wave Source for the Exact TF/SF Formulation	49
3.9	An Efficient Integer Mapping	52
3.10	Boundary Conditions and Vector Plane-Wave Polarization	55
3.11	Required Current Densities J_{inc} and M_{inc}	56
3.12	Summary of Method	59
3.13	Modeling Examples	59
3.14	Discussion	62
	References	62
4	Electromagnetic Wave Source Conditions	65
	<i>Ardavan Oskooi and Steven G. Johnson</i>	
4.1	Overview	65
4.2	Incident Fields and Equivalent Currents	65
4.2.1	The Principle of Equivalence	66
4.2.2	Discretization and Dispersion of Equivalent Currents	69
4.3	Separating Incident and Scattered Fields	70
4.4	Currents and Fields: The Local Density of States	73
4.4.1	The Maxwell Eigenproblem and the Density of States	74
4.4.2	Radiated Power and the Harmonic Modes	75
4.4.3	Radiated Power and the LDOS	78
4.4.4	Computation of LDOS in FDTD	78
4.4.5	Van Hove Singularities in the LDOS	80
4.4.6	Resonant Cavities and Purcell Enhancement	81
4.5	Efficient Frequency-Angle Coverage	83
4.6	Sources in Supercells	86
4.7	Moving Sources	89
4.8	Thermal Sources	92
4.9	Summary	95
	References	96
5	Rigorous PML Validation and a Corrected Unsplit PML for Anisotropic Dispersive Media	101
	<i>Ardavan Oskooi and Steven G. Johnson</i>	
5.1	Introduction	101
5.2	Background	102
5.3	Complex Coordinate Stretching Basis of PML	103
5.4	Adiabatic Absorbers and PML Reflections	104
5.5	Distinguishing Correct from Incorrect PML Proposals	105
5.6	Validation of Anisotropic PML Proposals	106
5.7	Time-Domain PML Formulation for Terminating Anisotropic Dispersive Media	108
5.8	PML Failure for Oblique Waveguides	110
5.9	Summary and Conclusions	112
	Acknowledgments	112
	Appendix 5A: Tutorial on the Complex Coordinate-Stretching Basis of PML	112
	5A.1 Wave Equations	113
	5A.2 Complex Coordinate Stretching	114
	5A.3 PML Examples	118
	5A.4 PML in Inhomogeneous Media	120
	5A.5 PML for Evanescent Waves	121

Appendix 5B: Required Auxiliary Variables	122
Appendix 5C: PML in Photonic Crystals	123
5C.1 Conductivity Profile of the pPML	123
5C.2 Coupled-Mode Theory	124
5C.3 Convergence Analysis	125
5C.4 Adiabatic Theorems in Discrete Systems	126
5C.5 Toward Better Absorbers	126
References	128
Selected Bibliography	132
6 Accurate FDTD Simulation of Discontinuous Materials by Subpixel Smoothing	133
<i>Ardavan Oskooi and Steven G. Johnson</i>	
6.1 Introduction	133
6.2 Dielectric Interface Geometry	134
6.3 Permittivity Smoothing Relation, Isotropic Interface Case	134
6.4 Field Component Interpolation for Numerical Stability	135
6.5 Convergence Study, Isotropic Interface Case	136
6.6 Permittivity Smoothing Relation, Anisotropic Interface Case	139
6.7 Convergence Study, Anisotropic Interface Case	140
6.8 Conclusions	142
Acknowledgment	143
Appendix 6A: Overview of the Perturbation Technique Used to Derive Subpixel Smoothing	143
References	147
7 Stochastic FDTD for Analysis of Statistical Variation in Electromagnetic Fields	149
<i>Steven M. Smith and Cynthia M. Furse</i>	
7.1 Introduction	149
7.2 Delta Method: Mean of a Generic Multivariable Function	150
7.3 Delta Method: Variance of a Generic Multivariable Function	151
7.4 Field Equations	154
7.5 Field Equations: Mean Approximation	155
7.6 Field Equations: Variance Approximation	156
7.6.1 Variance of the H -Fields	156
7.6.2 Variance of the E -Fields	157
7.7 Sequence of the Field and σ Updates	160
7.8 Layered Biological Tissue Example	161
7.9 Summary and Conclusions	164
Acknowledgment	164
References	164
8 FDTD Modeling of Active Plasmonics	167
<i>Ifrikhar Ahmed, Eng Huat Khoo, and Er Ping Li</i>	
8.1 Introduction	167
8.2 Overview of the Computational Model	168
8.3 Lorentz-Drude Model for Metals	168
8.4 Direct-Bandgap Semiconductor Model	170
8.5 Numerical Results	174

8.5.1 Amplification of a 175-fs Optical Pulse in a Pumped Parallel-Plate Waveguide	174
8.5.2 Resonance Shift and Radiation from a Passive Disk-Shaped GaAs Microcavity with Embedded Gold Nanocylinders	177
8.6 Summary	179
Appendix 8A: Critical Points Model for Metal Optical Properties	179
Appendix 8B: Optimized Staircasing for Curved Plasmonic Surfaces	181
References	182
Selected Bibliography	183

9 FDTD Computation of the Nonlocal Optical Properties of Arbitrarily Shaped Nanostructures

<i>Jeffrey M. McMahon, Stephen K. Gray, and George C. Schatz</i>	185
9.1 Introduction	185
9.2 Theoretical Approach	187
9.3 Gold Dielectric Function	189
9.4 Computational Considerations	191
9.5 Numerical Validation	191
9.6 Application to Gold Nanofilms (1-D Systems)	193
9.7 Application to Gold Nanowires (2-D Systems)	197
9.8 Application to Spherical Gold Nanoparticles (3-D Systems)	200
9.9 Summary and Outlook	202
Acknowledgments	203
Appendix 9A: Nonlocal FDTD Algorithm	203
References	205

10 Classical Electrodynamics Coupled to Quantum Mechanics for Calculation of Molecular Optical Properties: An RT-TDDFT/FDTD Approach

<i>Hanning Chen, Jeffrey M. McMahon, Mark A. Ratner, and George C. Schatz</i>	209
10.1 Introduction	209
10.2 Real-Time Time-Dependent Density Function Theory	211
10.3 Basic FDTD Considerations	213
10.4 Hybrid Quantum Mechanics/Classical Electrodynamics	213
10.5 Optical Property Evaluation for a Particle-Coupled Dye Molecule for Randomly Distributed Incident Polarization	214
10.6 Numerical Results 1: Scattering Response Function of a 20-nm-Diameter Silver Nanosphere	216
10.7 Numerical Results 2: Optical Absorption Spectra of the N3 Dye Molecule	219
10.7.1 Isolated N3 Dye Molecule	219
10.7.2 N3 Dye Molecule Bound to an Adjacent 20-nm Silver Nanosphere	220
10.8 Numerical Results 3: Raman Spectra of the Pyridine Molecule	222
10.8.1 Isolated Pyridine Molecule	222
10.8.2 Pyridine Molecule Adjacent to a 20-nm Silver Nanosphere	223
10.9 Summary and Discussion	227
Acknowledgment	228
References	228

11 Transformation Electromagnetics Inspired Advances in FDTD Methods

<i>Roberto B. Armenta and Costas D. Sarris</i>	233
11.1 Introduction	233
11.2 Invariance Principle in the Context of FDTD Techniques	234
11.3 Relativity Principle in the Context of FDTD Techniques	235
11.4 Computational Coordinate System and Its Covariant and Contravariant Vector Bases	236
11.4.1 Covariant and Contravariant Basis Vectors	236
11.4.2 Covariant and Contravariant Components of the Metric Tensor	237
11.4.3 Covariant and Contravariant Representation of a Vector	238
11.4.4 Converting Vectors to the Cartesian Basis and Vice Versa	239
11.4.5 Second-Rank Tensors in the Covariant and Contravariant Bases	239
11.5 Expressing Maxwell's Equations Using the Basis Vectors of the Computational Coordinate System	241
11.6 Enforcing Boundary Conditions by Using Coordinate Surfaces in the Computational Coordinate System	242
11.7 Connection with the Design of Artificial Materials	246
11.7.1 Constitutive Tensors of a Simple Material	246
11.7.2 Constitutive Tensors of an Artificial Material	247
11.8 Time-Varying Discretizations	249
11.9 Conclusion	252
References	252
Selected Bibliography	254

12 FDTD Modeling of Nondiagonal Anisotropic Metamaterial Cloaks

<i>Naoki Okada and James B. Cole</i>	255
12.1 Introduction	255
12.2 Stable FDTD Modeling of Metamaterials Having Nondiagonal Permittivity Tensors	256
12.3 FDTD Formulation of the Elliptic Cylindrical Cloak	256
12.3.1 Diagonalization	256
12.3.2 Mapping Eigenvalues to a Dispersion Model	258
12.3.3 FDTD Discretization	258
12.4 Modeling Results for an Elliptic Cylindrical Cloak	261
12.5 Summary and Conclusions	265
References	265

13 FDTD Modeling of Metamaterial Structures

<i>Costas D. Sarris</i>	269
13.1 Introduction	269
13.2 Transient Response of a Planar Negative-Refractive-Index Lens	270
13.2.1 Auxiliary Differential Equation Formulation	270
13.2.2 Illustrative Problem	271
13.3 Transient Response of a Loaded Transmission Line Exhibiting a Negative Group Velocity	274
13.3.1 Formulation	274
13.3.2 Numerical Simulation Parameters and Results	275
13.4 Planar Anisotropic Metamaterial Grid	277
13.4.1 Formulation	278
13.4.2 Numerical Simulation Parameters and Results	278
13.5 Periodic Geometries Realizing Metamaterial Structures	280

13.6	The Sine-Cosine Method	282
13.7	Dispersion Analysis of a Planar Negative-Refractive-Index Transmission Line	284
13.8	Coupling the Array-Scanning and Sine-Cosine Methods	285
13.9	Application of the Array-Scanning Method to a Point-Sourced Planar Positive-Refractive-Index Transmission Line	287
13.10	Application of the Array-Scanning Method to the Planar Microwave “Perfect Lens”	290
13.11	Triangular-Mesh FDTD Technique for Modeling Optical Metamaterials with Plasmonic Elements	292
13.11.1	Formulation and Update Equations	292
13.11.2	Implementation of Periodic Boundary Conditions	294
13.11.3	Stability Analysis	295
13.12	Analysis of a Sub-Wavelength Plasmonic Photonic Crystal Using the Triangular-Mesh FDTD Technique	297
13.13	Summary and Conclusions	302
	Acknowledgments	303
	References	303
	Selected Bibliography	306

14 Computational Optical Imaging Using the Finite-Difference Time-Domain Method

	<i>Ilker R. Capoglu, Jeremy D. Rogers, Allen Taflove, and Vadim Backman</i>	307
14.1	Introduction	307
14.2	Basic Principles of Optical Coherence	308
14.3	Overall Structure of the Optical Imaging System	309
14.4	Illumination Subsystem	310
14.4.1	Coherent Illumination	310
14.4.2	Incoherent Illumination	311
14.5	Scattering Subsystem	317
14.6	Collection Subsystem	319
14.6.1	Fourier Analysis	320
14.6.2	Green’s Function Formalism	326
14.7	Refocusing Subsystem	330
14.7.1	Optical Systems Satisfying the Abbe Sine Condition	331
14.7.2	Periodic Scatterers	337
14.7.3	Nonperiodic Scatterers	339
14.8	Implementation Examples: Numerical Microscope Images	344
14.8.1	Letters “N” and “U” Embossed on a Thin Dielectric Substrate	344
14.8.2	Polystyrene Latex Beads	346
14.8.3	Pair of Contacting Polystyrene Microspheres in Air	348
14.8.4	Human Cheek (Buccal) Cell	349
14.9	Summary	350
	Acknowledgment	350
	Appendix 14A: Derivation of Equation (14.9)	350
	Appendix 14B: Derivation of Equation (14.38)	351
	Appendix 14C: Derivation of Equation (14.94)	352
	Appendix 14D: Coherent Focused Beam Synthesis Using Plane Waves	353
	References	356

15 Computational Lithography Using the Finite-Difference Time-Domain Method

<i>Geoffrey W. Burr and Jaione Tirapu Azpiroz</i>	365
15.1 Introduction	365
15.1.1 Resolution	366
15.1.2 Resolution Enhancement	368
15.2 Projection Lithography	370
15.2.1 Light Source	371
15.2.2 Photomask	373
15.2.3 Lithography Lens	377
15.2.4 Wafer	378
15.2.5 Photoresist	378
15.2.6 Partial Coherence	380
15.2.7 Interference and Polarization	381
15.3 Computational Lithography	384
15.3.1 Image Formation	384
15.3.2 Mask Illumination	393
15.3.3 Partially Coherent Illumination: The Hopkins Method	398
15.3.4 Image in Resist Interference	400
15.4 FDTD Modeling for Projection Lithography	401
15.4.1 Basic FDTD Framework	402
15.4.2 Introducing the Plane-Wave Input	404
15.4.3 Monitoring the Diffraction Orders	406
15.4.4 Mapping onto the Entrance Pupil	408
15.4.5 FDTD Gridding	411
15.4.6 Parallelization	412
15.5 Applications of FDTD	414
15.5.1 Electromagnetic Field Impact of Mask Topography	414
15.5.2 Making TMA More Electromagnetic-Field Aware	416
15.5.3 Hopkins Approximation	420
15.6 FDTD Modeling for Extreme Ultraviolet Lithography	423
15.6.1 EUVL Exposure System	423
15.6.2 EUV Reticle	426
15.6.3 EUVL Mask Modeling	427
15.6.4 Hybrid Technique Using Fourier Boundary Conditions	432
15.7 Summary and Conclusions	433
Appendix 15A: Far-Field Mask Diffraction	434
Appendix 15B: Debye's Representation of the Focusing Fields	435
Appendix 15C: Polarization Tensor	438
Appendix 15D: Best Focus	440
References	442

16 FDTD and PSTD Applications in Biophotonics

<i>Ilker R. Capoglu, Jeremy D. Rogers, César Méndez Ruiz, Jamesina J. Simpson, Snow H. Tseng, Kun Chen, Ming Ding, Allen Taflove, and Vadim Backman</i>	451
16.1 Introduction	451
16.2 FDTD Modeling Applications	452
16.2.1 Vertebrate Retinal Rod	452
16.2.2 Angular Scattering Responses of Single Cells	453
16.2.3 Precancerous Cervical Cells	454

16.2.4	Sensitivity of Backscattering Signatures to Nanometer-Scale Cellular Changes	458
16.2.5	Modeling Mitochondrial Aggregation in Single Cells	459
16.2.6	Focused Beam Propagation through Multiple Cells	461
16.2.7	Computational Imaging and Microscopy	463
16.2.8	Detection of Nanometer-Scale z -Axis Features within HT-29 Colon Cancer Cells Using Photonic Nanojets	471
16.2.9	Assessment of the Born Approximation for Biological Media	476
16.3	Overview of Fourier-Basis PSTD Techniques for Maxwell's Equations	478
16.4	PSTD and SL-PSTD Modeling Applications	479
16.4.1	Enhanced Backscattering of Light by a Large Cluster of 2-D Dielectric Cylinders	479
16.4.2	Depth-Resolved Polarization Anisotropy in 3-D Enhanced Backscattering	481
16.4.3	Sizing Spherical Dielectric Particles in a 3-D Random Cluster	486
16.4.4	Optical Phase Conjugation for Turbidity Suppression	489
16.5	Summary	492
	References	492

17 GVADE FDTD Modeling of Spatial Solitons

	<i>Zachary Lubin, Jethro H. Greene, and Allen Taflove</i>	497
17.1	Introduction	497
17.2	Analytical and Computational Background	497
17.3	Maxwell-Ampere Law Treatment of Nonlinear Optics	498
17.4	General Vector Auxiliary Differential Equation Method	501
17.4.1	Lorentz Linear Dispersion	501
17.4.2	Kerr Nonlinearity	502
17.4.3	Raman Nonlinear Dispersion	502
17.4.4	Solution for the Electric Field	504
17.4.5	Drude Linear Dispersion for Metals at Optical Wavelengths	505
17.5	Applications of GVADE FDTD to TM Spatial Soliton Propagation	506
17.5.1	Single Narrow Fundamental TM Spatial Soliton	507
17.5.2	Single Wide Overpowered TM Spatial Soliton	508
17.5.3	Interactions of Co-Propagating Narrow TM Spatial Solitons	508
17.6	Applications of GVADE FDTD to TM Spatial Soliton Scattering	511
17.6.1	Scattering by a Square Sub-Wavelength Air Hole	511
17.6.2	Interactions with Thin Plasmonic Gold Films	512
17.7	Summary	515
	References	516

18 FDTD Modeling of Blackbody Radiation and Electromagnetic Fluctuations in Dissipative Open Systems

	<i>Jonathan Andreasen</i>	519
18.1	Introduction	519
18.2	Studying Fluctuation and Dissipation with FDTD	519
18.3	Introducing Blackbody Radiation into the FDTD Grid	520
18.4	Simulations in Vacuum	523
18.5	Simulations of an Open Cavity	526
18.5.1	Markovian Regime ($\tau \gg \tau_c$)	526
18.5.2	Non-Markovian Regime ($\tau \sim \tau_c$)	528
18.5.3	Analytical Examination and Comparison	530
18.6	Summary and Outlook	531
	References	532

19 Casimir Forces in Arbitrary Material Geometries	535
<i>Ardavan Oskooi and Steven G. Johnson</i>	
19.1 Introduction	535
19.2 Theoretical Foundation	536
19.2.1 Stress-Tensor Formulation	536
19.2.2 Complex Frequency Domain	537
19.2.3 Time-Domain Approach	538
19.2.4 Expression for the Casimir Force as a Time-Domain Integration	541
19.2.5 Evaluation of $g(-t)$ in (19.28)	542
19.3 Reformulation in Terms of a Harmonic Expansion	544
19.4 Numerical Study 1: A 2-D Equivalent to a 3-D Configuration	545
19.5 Numerical Study 2: Dispersive Dielectric Materials	548
19.6 Numerical Study 3: Cylindrical Symmetry in Three Dimensions	550
19.7 Numerical Study 4: Periodic Boundary Conditions	552
19.8 Numerical Study 5: Fully 3-D FDTD-Casimir Computation	553
19.9 Generalization to Nonzero Temperatures	556
19.9.1 Theoretical Foundation	556
19.9.2 Incorporating $T > 0$ in the Time Domain	557
19.9.3 Validations	558
19.9.4 Implications	559
19.10 Summary and Conclusions	560
Acknowledgments	560
Appendix 19A: Harmonic Expansion in Cylindrical Coordinates	561
References	562
20 Meep: A Flexible Free FDTD Software Package	567
<i>Ardavan Oskooi and Steven G. Johnson</i>	
20.1 Introduction	567
20.1.1 Alternative Computational Tools	568
20.1.2 The Initial-Value Problem Solved by Meep	568
20.1.3 Organization of This Chapter	569
20.2 Grids and Boundary Conditions	570
20.2.1 Coordinates and Grids	570
20.2.2 Grid Chunks and Owned Points	570
20.2.3 Boundary Conditions and Symmetries	572
20.3 Approaching the Goal of Continuous Space-Time Modeling	573
20.3.1 Subpixel Smoothing	573
20.3.2 Interpolation of Field Sources	576
20.3.3 Interpolation of Field Outputs	578
20.4 Materials	578
20.4.1 Nonlinear Materials	579
20.4.2 Absorbing Boundary Layers: PML, Pseudo-PML, and Quasi-PML	579
20.5 Enabling Typical Computations	581
20.5.1 Computing Flux Spectra	581
20.5.2 Analyzing Resonant Modes	582
20.5.3 Frequency-Domain Solver	583
20.6 User Interface and Scripting	586
20.7 Abstraction Versus Performance	588
20.7.1 Primacy of the Inner Loops	589
20.7.2 Time-Stepping and Cache Trade-Offs	589

20.7.3 The Loop-in-Chunks Abstraction	591
20.8 Summary and Conclusions	592
Acknowledgments	592
References	592
Acronyms and Common Symbols	597
About the Authors	601
Index	611